JOURNAL OF SPACECRAFT AND ROCKETS
Vol. 36, No. 5, September–October 1999

Radar and Optical Characterization of an Anomalous Orbital Debris Population

R. Sridharan,* W. Beavers,† E. M. Gaposchkin,‡ R. Lambour,§ and J. Kansky§
Lincoln Laboratory, Massachusetts Institute of Technology, Lexington, Massachusetts 02420-9185
and
E. Stansbery¶
NASA Johnson Space Center, Houston, Texas 77058

Analysis of orbital debris data collected by the Haystack radar have shown an anomalously high concentration of debris between the altitudes of 800 and 1000 km. Indications from the Haystack data are that the debris range in size from 8 mm to 2 cm and that they are spherical in shape. Previous work by NASA researchers has shown the likely origin to be the leaking of liquid coolant from the nuclear power sources of a now defunct Soviet space-based series of ocean surveillance satellites. We report on a project at Massachusetts Institute of Technology's Lincoln Laboratory to detect, track, and characterize a small sample of the anomalous debris using ground-based radars and telescopes. Our goal was to provide evidence supporting or refuting the NASA conclusions. We have determined that the size, shape, density, and surface properties of the debris are consistent with the hypothesis that it is liquid, eutectic sodium–potassium coolant like that used in the Soviet satellites. The techniques used to detect and track the debris are discussed. The radar and optical data used to characterize the debris are also presented.

Nomenclature

A	= projected area of object, m^2
a	= radius of spherical radar target, m
C_d	= ballistic coefficient
F_{drag}	= atmospheric drag force acting on an orbiting object
I_1 (I_2)	= intensity of light polarized in the plane parallel (perpendicular) to the plane of incidence
k	= complex index of refraction (attenuation coefficient)
M	= mass of object subjected to atmospheric drag, g
$M1$	= astronomical V-band visual magnitude corrected to a range of 1000 km
n	= real index of refraction
r	= reflectivity (albedo)
S_d	= thermospheric density scale factor for debris object
S_0	= thermospheric density scale factor for radar calibration sphere
V_s	= velocity of an object relative to the atmospheric velocity
V_{sun}	= astronomical V-band visual magnitude of the sun (−26.8)
λ	= wavelength, m
ρ_{true} (ρ_{model})	= true (modeled) thermospheric density
σ	= radar cross section of spherical target, dBsm, dB relative to a square meter
Φ	= phase function
ϕ	= phase angle (sun–object–observer angle), deg or rad

Received 5 August 1997; revision received 30 September 1998; accepted for publication 4 October 1998.

* Senior Staff Member, Surveillance Techniques Group, 244 Wood Street. Member AIAA.
† Staff Member and Consultant, Surveillance Techniques Group, 244 Wood Street.
‡ Senior Staff and Consultant, Surveillance Techniques Group, 244 Wood Street.
§ Staff Member, Surveillance Techniques Group, 244 Wood Street.
¶ Scientist, Orbital Debris Program Office, Earth Science and Solar System Exploration Division.

Introduction

OVER the past two decades, there has been increasing interest in the specification and characterization of the orbital debris environment, driven by the potential of significant damage to crewed spacecraft due to collision with such debris. The typical impact velocity in low Earth orbit would be ~10 km/s, which means that even very small pieces of debris could produce catastrophic damage. Therefore, the short- and long-term safety of spacecraft are dependent on obtaining an adequate understanding of the current debris environment and its temporal evolution.

Knowledge of the debris environment was previously split over two size regimes. Objects larger than ~10 cm in diameter are cataloged by the U.S. Space Command (USSPACECOM) Space Surveillance Network's ground-based radars. Orbital elements, radar cross section, and information on the origin of each object are maintained in the catalog. The analysis of surfaces exposed to impacts, such as the long-duration exposure facility (LDEF) or the European retrievable carrier (EURECA), and data returned from active impact experiments, such as the Interplanetary Dust Experiment on LDEF, have provided all of the data on debris with diameters less than ~0.1 cm. The lack of data in the 0.1–10 cm size regime prompted NASA to sponsor radar measurements of the debris environment using the Haystack radar operated by the Massachusetts Institute of Technology (MIT) Lincoln Laboratory in Westford, Massachusetts.[1,2] Haystack is a high-power, X-band radar operating at 10 GHz, with a 1-mrad field of view. The single-pulse signal-to-noise ratio (SNR) for a 1-m^2 target at a range of 1000 km is 58 dB. Haystack can observe objects as small as 1 cm in diameter at a range of 1000 km and is well suited for obtaining data in the 0.3–10 cm regime.

The radar is operated in a stare mode for debris data collection, i.e., the radar is pointed at an azimuth and elevation over a slant range extent. The Earth's rotation creates a scan of space. Data are recorded whenever a preset threshold SNR for detection is exceeded. These data are processed by NASA and provide cumulative statistics of detection as well as orbit and size characterization. One method of presenting the results is shown in Fig. 1, which is adapted from Ref. 2. Figure 1 represents the rate of detections in the Haystack beam when pointed at zenith as a function of the altitude of detection. The lower curve is a simulation of the rate for the known catalog carried by the U.S. Air Force's Space Surveillance Center, whereas the upper curve is the rate of detections processed from the Haystack data. NASA estimates that the total rate across all altitudes sampled (<1500 km) is ~6.25 objects/h.

Table 1 Characteristics of radars used in this study

Radar	Band	Frequency, GHz	Field of view, mrad	SNR on 1-m^2 target at 1000 km, dB
Haystack (Westford, MA)	X	10	1	58
Millstone (Westford, MA)	L	1.3	8	50
TRADEX (Kwajalein Atoll)	L	1.3	8	48

Table 2 Characteristics of optical sensors used in this study

Telescope	Aperture, m	Sensor	Field of view, deg	Sensitivity (magnitude)
Firepond (Westford, MA)	1.2	CCD photopolarimeter	0.06	$\sim 13 m_v$
ETS (Soccoro, NM)	0.75	Vidicon camera	1–2	$15–17 m_v$

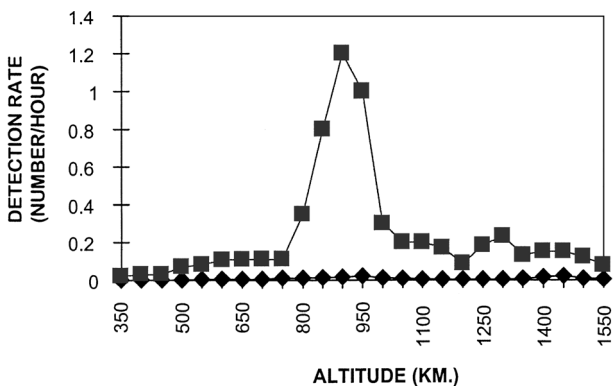

Fig. 1 Comparison of observed (■) and cataloged (♦) debris detection rates.

Most of the debris detections shown in Fig. 1 are concentrated in the altitude range between 800 and 1000 km though there is a noticeable but smaller peak at ~1400 km. We only consider the debris in the 800–1000-km region. Analysis of these detections by NASA has led to the following conclusions[3]:

1) The debris are primarily small (<2-cm diameter) and largely spherical in shape.

2) The debris are concentrated in circular orbits with inclination of ~65 deg at altitudes of 900–1000 km.

3) The debris are likely to be leaked liquid sodium–potassium (NaK) coolant from the Bouk class of nuclear power sources used on Soviet Radar Ocean Reconnaissance Satellites (RORSATs),[‡] which were placed into similar orbits for long-term storage.

4) There are 50,000–70,000 such debris >8 mm in size at these altitudes, and these constitute approximately half the total debris population below 1500-km altitude.

This band of debris is termed anomalous debris because the debris density exceeded theoretical models by a significant factor.

NASA funded an effort at Lincoln Laboratory to detect, track, and characterize a sample set of the anomalous debris objects. Whereas NASA's analysis used detection data of large numbers of debris in this band, we attempted to characterize in detail a small number of representative samples from this band using the radar and optical sensors operated by MIT Lincoln Laboratory. These sensors are located at Westford, Massachusetts; Kwajalein Atoll, Marshall Islands; and Socorro, New Mexico. The characteristics of each sensor are presented in Tables 1 and 2. The purpose of the effort was to provide evidence supporting or refuting the conclusions arrived at by NASA. This paper presents examples of radar and optical observations of the anomalous debris and the characteristics derived from the data. The derived characteristics include orbital parameters, shape and size of the debris, surface characteristics at visible wavelengths, and the mass and density of the debris. A companion paper investigates the thermal properties and orbital lifetime of the debris based on the characteristics derived in this paper.

[‡]Russian Institute of Physics and Power Engineering Web site, http://www.rssi.ru/ippe/general/spacer.html.

Debris Detection Strategies

Before detailed characterization of the debris could begin, candidate objects had to be acquired. Three different strategies were used for the detection and acquisition of anomalous debris objects with the radars. These were 1) search in the orbit of putative parent satellites, 2) stare and chase using optical systems and radars, and 3) search of the orbit planes of previously detected anomalous debris objects.

Search of Orbits of Putative Parent Objects

The properties of the radars used in this effort are summarized in Table 1. The suspected parent satellites for the anomalous debris are the ejected RORSAT nuclear reactor cores mentioned in the preceding section. Millstone hill radar (MHR) (Westford, Massachusetts) searched the orbits of 10 putative parent objects with each search being centered about the parent. Despite this search mode being capable of detecting an ~2-cm-diam object if coherently trackable and an ~3.5-cm-diam object if tracked noncoherently, no detections resulted. If there were any recent slow leaks of coolant from these reactor cores the orbit planes of the droplets and the parents would have been close together. Therefore, we believe that none of the putative parent objects whose orbits were searched had leaked debris of size ≥2 cm diameter within ~30 days of the search.

Stare and Chase

The experimental electro-optical test system (ETS) located in New Mexico is an optical system that was a proof of concept for the ground-based electro-optical deep space surveillance system. The ETS has two telescopes, the properties of which are summarized in Table 2. The system is capable of detecting a resident space object, correlating it against the catalog, and if uncorrelated, transitioning from stare to tracking the object in near-real time.[4] The ETS conducted several stare-and-chase sessions for debris in 1994. One anomalous debris was found and has been characterized extensively.[5]

The target resolution and discrimination experiment (TRADEX) radar (Kwajalein Atoll) also conducted several stare and chase sessions during 1995. The properties of the radar are summarized in Table 1. The operating principle for TRADEX is the same as for ETS. The radar points at a specific azimuth and a specific high elevation and examines a range between 500 and 1200 km. The radar's sensitivity is such that it should detect any object >3.5 cm in diameter in this altitude range.[6] The radar found four anomalous debris objects.

Search of Debris Orbit Planes

If the anomalous debris were a result of the leaking of a liquid, there would be many droplets per orbit plane. Hence, the orbit planes of the debris found by ETS and TRADEX were searched with the MHR. Millstone found six more anomalous debris objects. Finally, the Haystack radar also searched some of the debris orbits. Haystack found eight more debris objects though, unlike the 11 debris objects found earlier, these were not completely characterized.

A key finding of this study is that there are multiple debris per orbit plane, which implies a common parentage and time of origin for the debris consistent with the hypothesis of a leaking liquid.

Radar Data and Analysis

MHR and Haystack collected a significant amount of data on the 11 debris objects found during the searches. These data include radar signatures (time history of radar cross sections) to estimate size and assess temporal variability and/or spin periods, polarization data to infer the shape of the debris, and metric data to support determination of orbits, calculation of area-to-mass ratios, and mass and densities for the debris. Each of these topics will be discussed. The orbital parameters for the debris are presented in Table 3.

Radar Signature and Polarization Data

MHR transmits a right circularly polarized electromagnetic wave toward a target. For the return signal, the principal polarization (PP) is consequently left circularly polarized and the orthogonal

polarization (OP) is right circular. The radar's tracking program dynamically selects the number of pulses integrated per signal processing cycle based on the SNR required for accurate metric tracking.

Figure 2 is representative of the radar signature data on the anomalous debris recorded at the MHR during a track. Tracks typically last 10 min, and we have a number of tracks on each object (cf. Table 4). For the sake of brevity, we do not present all of our data. Figure 2 presents a temporal history of the PP and OP radar cross sections (RCS) in decibels relative to a square meter (dBsm) (essentially the difference between the target and a 1 m^2 target; e.g., a 0.1 m^2 target will have an RCS of −10 dBsm) for approximately 100 s. The radar does not detect any temporal variation in the PP RCS at a period longer than the integration interval (1–3 s) for either object. The OP RCS is typically below the PP RCS by ∼25 dB, as in Fig. 2. The structure in the OP RCS is actually dominated by noise (the gaps in the OP return represent periods when the return dropped below the lower scale on the plot; i.e., the OP return was at the noise level). A number of tracks have been taken at a variety of aspect angles, and all show the same structure. This behavior is quite unusual for debris. Over 300 tracks of other (nonanomalous) debris have been accumulated by the MHR, and all show that the OP/PP ratio is commonly on the order of a few decibel and varies over the course of the

Table 3 Orbital parameters for anomalous debris

Object number	Inclination, deg	Eccentricity	Right ascension, deg	Semimajor axis R_E
81215	64.96	0.004	304.38	1.146
33562	65.04	0.004	77.291	1.146
33609	64.96	0.005	203.35	1.146
33612	64.97	0.005	187.93	1.146
33616	64.69	0.006	207.65	1.147
39969	64.69	0.006	222.31	1.147
39970	64.65	0.006	207.86	1.147
39971	64.96	0.004	300.13	1.146
39972	64.97	0.005	202.81	1.146
39973	65.05	0.004	86.32	1.146
39974	65.06	0.004	152.82	1.145

Table 4 Millstone radar results

Object number	Number of tracks	⟨PP RCS⟩, dBsm	Polarization ratio, dB	Radius, cm	Sigma, cm
81215	51	−20.8	−24.2	2.84	0.09
33562	45	−23.6	−21.6	2.55	0.06
33609	30	−22.4	−23.3	2.68	0.08
33612	23	−22.1	−25.3	2.71	0.05
33616	25	−30.7	−25.1	1.94	0.09
39969	12	−34.3	−21.2	1.70	0.08
39970	10	−32.3	−25.2	1.83	0.02
39971	4	−21.9	−24.5	2.73	0.03
39972	5	−22.1	−24.0	2.70	0.02
39973	3	−25.4	−21.2	2.38	——
39974	1	−25.0	−25.0	——	——

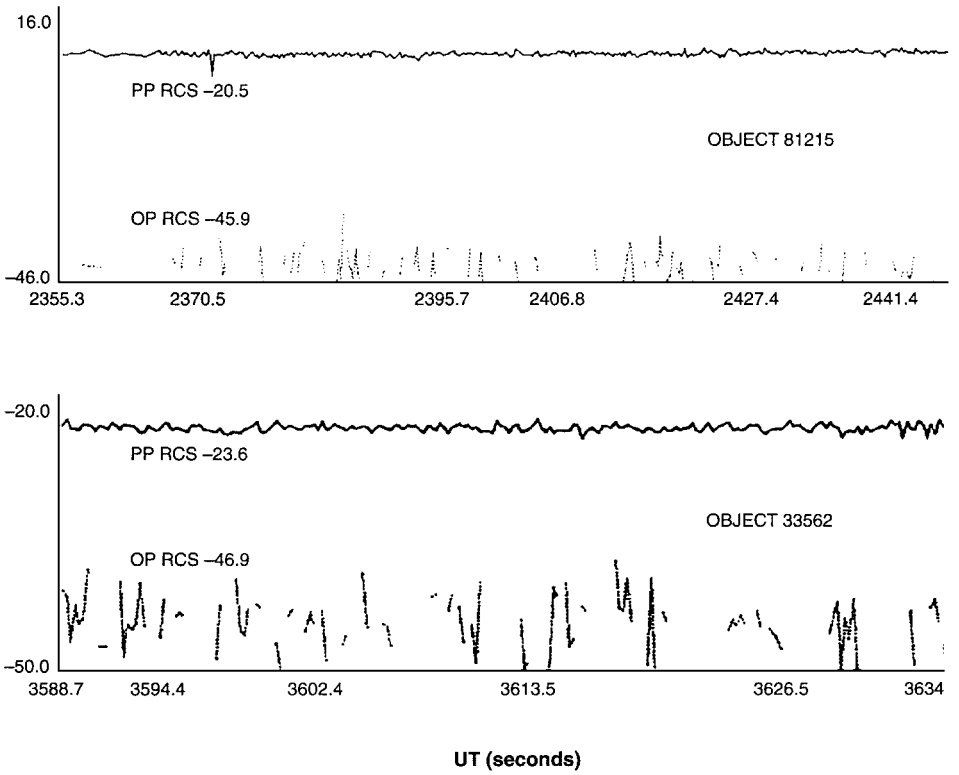

Fig. 2 Millstone L-band PP and OP RCS data for two anomalous debris pieces.

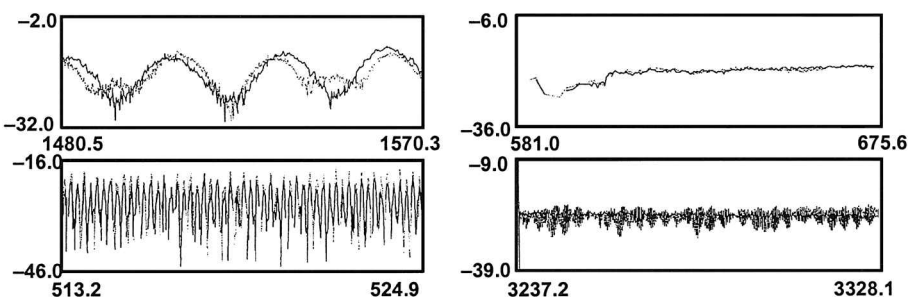

Fig. 3 Millstone L-band PP (——) and OP (– – –) radar signatures for four nonanomalous debris pieces; *x* axis displays universal time (UT) in seconds, and the *y* axis shows RCS in dBsm; data are representative of the variations observed in the radar signatures of most orbital debris.

track.[7] Figure 3 presents RCS measurements as a function of time for four nonanomalous debris to illustrate this point.

In Fig. 4 we compare the PP and OP RCS for one of the anomalous debris objects with the RCS of Lincoln calibration sphere 4 (LCS-4). LCS-4 is a polished rigid aluminum sphere with radius 56.469 cm and projected area of 1 m^2, which was designed for radar calibration. It is well known that the OP return from a spherical object is negligible compared to the PP return over all aspect angles for a circularly polarized electromagnetic transmission. The anomalous debris display the same properties as the calibration sphere: invariant PP RCS over all aspect angles and very low OP RCS. Thus, we infer that the anomalous debris are spherical in shape. The mean PP RCS for the debris, the polarization ratio (defined as the mean OP RCS − PP RCS), the estimated radii, and the uncertainties are presented in Table 4.

We can infer the size of the anomalous debris from the PP RCS. We note that the PP RCS is consistently small enough so that the ratio of target size to radar wavelength is well in the Rayleigh scattering region for the radar, and there is no ambiguity in estimating the size from the RCS. The OP RCS is consistently down at the noise level. We assume that the debris are perfectly conducting so that the relation between RCS and radius may be written as[8]

$$\sigma/\pi a^2 = 9(2\pi a/\lambda)^4 \tag{1}$$

The uncertainties are based on the variability of the estimated mean RCS in the PP channel. The RCS estimate at the MHR is accurate to <1 dBsm based on frequent tracks of LCS-4. The same calibration uncertainty should apply to the small spheres in question because the radar attempts to track all objects at approximately the same SNR (30–36 dB). This high SNR is achievable in the case of the small spheres because of the high sensitivity of and the low slant range from the radar.

Density Estimation

The Earth's atmosphere extends beyond the 800–1000-km altitude at which the anomalous debris reside. Therefore, with accurate metric data over many orbits, it is feasible to estimate an area-to-mass ratio for the objects using the effects of atmospheric drag. Given that the debris are spherical, the area/mass ratio does not depend on aspect angle. The area and volume of the debris can be computed using the parameters in Table 4, leading to estimates of the mass and density.

The force on the debris due to drag is expressed as

$$\bar{F}_{\text{drag}} = -\tfrac{1}{2} C_d (A/M) \rho V_s \bar{V}_s \tag{2}$$

The approach taken here is that C_d, the shape of the debris, ρ, and V_s are assumed as known and that A/M is to be determined using the tracking data. The thermospheric density is provided by the mass spectrometer and incoherent scatter (MSIS83) thermosphere model,[9] and the Earth's atmosphere is assumed to be corotating to facilitate computation of V_s.

The thermosphere models are known to have errors ranging from 15 to 30% for use in drag analysis.[10–12] We correct for this error by introducing a scale factor S_0 for the thermospheric density so that $\rho_{\text{true}} = S_0 \rho_{\text{model}}$. To determine S_0, we utilize contemporaneous tracking data on LCS-4, which is at a similar altitude. LCS-4 is a well-characterized sphere, which facilitates accurate calculation of its ballistic coefficient (~2.2 for a sphere) and the drag force. A value for S_0 is determined using the tracking data, and it is then used to correct the thermospheric density.

Values of A/M for the debris are calculated with the aid of a precision orbit determination code called DYNAMO. DYNAMO uses an iterative weighted least-squares method to fit the radar tracking data. The code consists of an atmospheric drag model, a full geopotential model, models for lunar and solar perturbations, body and ocean tides, solar radiation pressure, Earth-reflected albedo pressure, and general relativity.[10] In calculating the drag force, DYNAMO introduces a multiplicative drag scale factor S_d (not to be confused with S_0) into Eq. (2). S_d is solved for during the tracking data fit and is representative of the error in the thermosphere model. If S_d is greater (less) than unity, the thermosphere model density is too small (large). For each of the anomalous debris, an initial value is assumed for A/M; that is, $(A/M)_{\text{initial}} = 0.1$ cm^2/g. S_d is then calculated for intervals with sufficient tracking data. The scale factor derived from contemporaneous LCS-4 tracking data is introduced, and the drag force may be expressed as

$$\bar{F}_{\text{drag}} = -\tfrac{1}{2} S_d (A/M)_{\text{initial}} C_d (\rho_{\text{true}}/S_0) V_s \bar{V}_s \tag{3}$$

The true value of A/M can then be estimated from

$$A/M = (S_d/S_0)(A/M)_{\text{initial}} = 0.1(S_d/S_0) \tag{4}$$

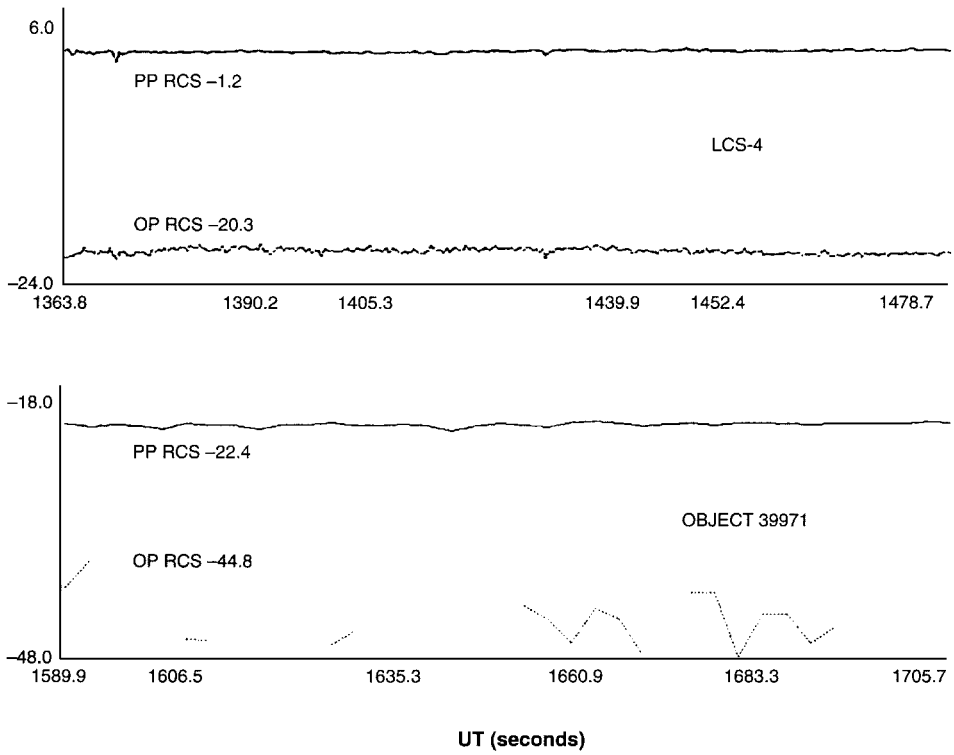

Fig. 4 Comparison of Millstone L-band radar signatures for a radar calibration sphere LCS-4 and one of the anomalous debris pieces, object 39971.

The mass and density of the debris then follow. Table 5 presents the results of this calculation for 9 of the 11 anomalous debris (2 did not have sufficient tracking data). The mean density of the debris is 1.03 ± 0.05 g/cm^3. The uncertainties are computed from the variation in the individual calculations.

Reference 4 indicated that eutectic NaK was probably used as the coolant in the nuclear power sources of the Soviet satellites that are the suspected parents of these debris. On the assumption that the anomalous debris are composed of NaK, we looked up standard chemical tables for the density. Figure 5 gives the variation of density of eutectic NaK with temperature.[13] It is clear that the expected density of eutectic NaK at ~300 K is 0.9 g/cm^3, similar to the derived density of the anomalous debris.

Several caveats are warranted. In the 800-km-altitude regime, the errors in the determination of C_d are on the order of $\pm 10\%$. In addition, the theory behind the calculation of C_d depends on the scattering mechanism, and there are no measurements of the scattering of atmospheric constituents off liquids.[14] For example, if the particles did not scatter but instead were absorbed, $C_d = 1.0$, which would increase A/M by 2.2 and decrease the mass and density. Last, the uncertainty in the determination of radius from RCS also affects this calculation.

Table 5 Anomalous debris mass and density estimates from MHR

Object number	A/M, cm^2/g	N	Mass, g	Density, g/cm^3
81215	0.253 ± 0.007	31	100.2 ± 9.1	1.044 ± 0.06
33562	0.273 ± 0.066	6	74.8 ± 9.6	1.077 ± 0.11
33609	0.225 ± 0.011	7	100.2 ± 10.8	1.244 ± 0.10
33612	0.256 ± 0.006	5	90.1 ± 5.4	1.031 ± 0.04
33616	0.349 ± 0.009	6	33.8 ± 4.0	1.108 ± 0.08
39969	0.464 ± 0.22	3	19.6 ± 3.0	0.953 ± 0.09
39970	0.545 ± 0.043	2	19.3 ± 2.1	0.752 ± 0.07
39971	0.247	1	94.8	1.112
39972	0.307	1	74.6	0.905

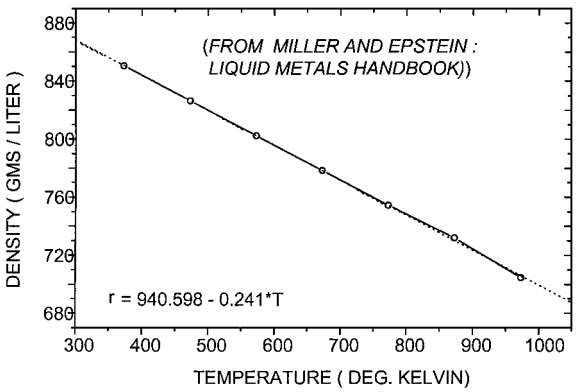

Fig. 5 Density of eutectic NaK alloy (77.8% K, 22.2% Na by weight[13]) as a function of temperature; equation represents a linear fit to the data points.

Optical Data and Analysis

Optical telescopes with appropriate instrumentation can also be used to determine some of the physical properties of orbital debris by examining the reflected sunlight. We have utilized the telescopes at the ETS and those at the Firepond facility collocated with the Millstone and Haystack radars. These telescope systems are briefly described in Table 2. Because the work at ETS involved only one of the anomalous debris (81215), and has been documented elsewhere,[5] we concentrate on the measurements taken on seven of the anomalous debris objects at Firepond.

The Firepond telescope has a small field of view, which usually makes acquiring, and tracking the anomalous debris challenging. However, there exists a real-time link between Firepond, Millstone, and Haystack that allows the radars to guide the pointing to the telescope, thus permitting data collection over a wide range of phase angles.

The sensor employed at Firepond is a combination charge-coupled device (CCD) photometer/polarimeter mounted at the focal plane of the telescope. Three elements are in the optical path, the first of which is a rotating filter wheel containing a set of standard UVBRI astronomical filters.[15] The V filter (~480–700 nm) was used in this study. The second element is a half-wave plate. This is a birefringent material, which introduces a 90-deg phase difference in the ordinary and extraordinary wave components of the light passed through it so that they emerge orthogonally polarized.[16] The third element is a Savart plate, which spatially separates the two orthogonal polarizations, producing two images on the CCD. In practice, sunlight reflected by orbiting objects will be partially linearly polarized in the plane perpendicular to the plane of incidence containing the sun, observer, and object. Proper rotation of the half-wave plate during an observation will cause the two images to correspond to the polarizations in the plane of incidence and perpendicular to that plane. This allows determination of the percentage polarization (% POL) of the reflected sunlight from the brightness of the two images:

$$\%\,\mathrm{POL} = 100 \times \frac{(I_1 - I_2)}{(I_1 + I_2)} \tag{5}$$

where I_1 and I_2 are the mesured intensities in the two planes and the photometric brightness of the image, $I = (I_1 + I_2)$. The photopolarimeter measurements are calibrated by observing photometric and polarimetric standard stars during each observing session. The observed counts are then transformed to V-band magnitudes, and the magnitude is normalized to a constant range of 1000 km.

Photometry

The predicted brightness of a solar illuminated object is given by[17]

$$M1 = V_{\mathrm{sun}} - 2.5 \log[rA\Phi(\phi)] \tag{6}$$

Figure 6 displays photometric phase curves for two of the anomalous debris. It can be clearly seen that the phase functions are fairly

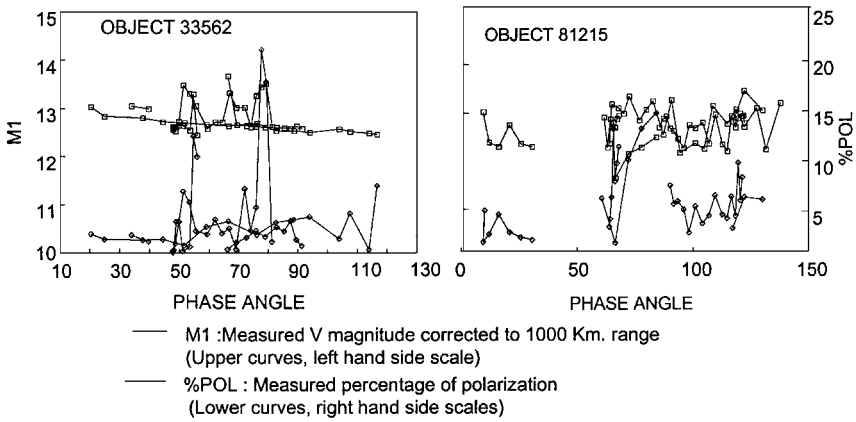

Fig. 6 Photometric (visual band magnitude at 1000-km range vs phase angle) and polarimetric (% polarization vs phase angle) phase curves for two of the anomalous debris with *y*-axis scale for the photometric (polarimetric) phase curve is on the left (right).

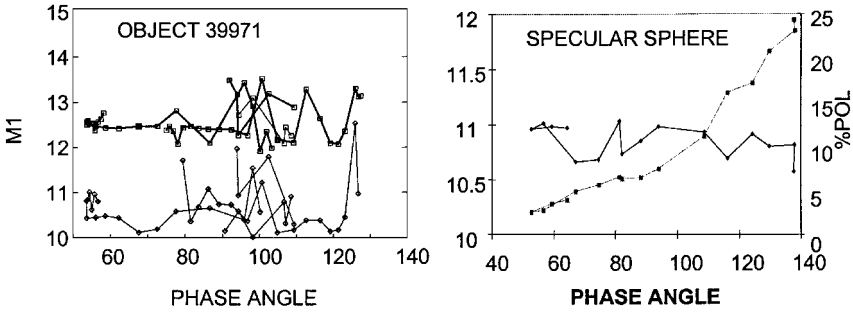

Fig. 7 Photometric and polarimetric phase curves (format as in Fig. 6) for amonalous debris object 39971 and specular sphere LCS-4.

Table 6 Summary of size estimates from optical measurements

Object number	$M1$	r	Radius, cm
81215	12.6 ± 0.4	0.89	2.9 ± 0.5
33562	12.8 ± 0.3	0.89	2.6 ± 0.4
33609	12.5 ± 0.2	0.84	3.0 ± 0.3
39969	13.6 ± 0.08	0.89	1.8 ± 0.1
39970	13.5 ± 0.2	0.89	1.8 ± 0.5
39971	12.6 ± 0.4	0.89	2.9 ± 0.5
39972	12.7 ± 0.3	0.84	2.9 ± 0.4

flat (with some noise due to low count rates) over all phase angles, which is typical for the seven anomalous debris pieces, and very atypical of other (nonanomalous) known debris obeserved by Firepond. A flat photometric phase curve is characteristic of a specularly reflecting sphere; its phase function is $\Phi = (4\pi)^{-1}$. Figure 7, presented for comparison, shows the photometric phase curve for an anomalous debris and a known specular sphere, one of the Lincoln radar calibration spheres. The phase curves are similar in shape.

Polarimetry

The polarization measurements can be used to determine the reflectivity of the anomalous debris pieces. The reflected light is partially linearly polarized in the plane perpendicular to the sun–object–observer plane by an amount that depends on the optical indices of the debris surface material. Therefore, a polarimetric phase curve can be constructed and fit to the Fresnel equations[16] for reflection to obtain a pair of optical indices (n, k). It is assumed that the angles of incidence and reflection are equal to half the observed phase angle. Figures 6 and 7 also show examples of the polarimetric phase curves for the anomalous debris (Fig. 6) and the specular sphere (Fig. 7). The anomalous debris typically show very low polarization at all phase angles (with some variations due to low count rates or variable air mass), which is characteristic of a metallic surface. The normal reflectivity of the object may be computed from the following relation[16]:

$$r = \left[\frac{(n-1)^2 + k^2}{(n+1)^2 + k^2}\right] \tag{7}$$

The values of (n, k) derived from the fits to the phase curve are not necessarily unique, but all values of (n, k) that do fit the measurements produce similar values of r (<1% scatter). Comparison of polarimetric data taken on the anomalous debris pieces with polarimetric phase curves for liquid metals known to be used as nuclear reactor coolants in the Soviet Union, e.g., see earlier footnote, shows that sodium, potassium, and lithium are the only metals whose polarization properties are similar to those of the anomalous debris. We were unable to locate any measurements of the indices of refraction of solid or liquid NaK in the literature, which would have allowed a direct comparison.

Once the phase function and reflectivity of the anomalous debris have been estimated, Eq. (6) is inverted to obtain A and the radius of the objects. Note that we assume that the debris are spherical and use the phase function for a specular sphere. The results of this analysis are presented in Table 6. The radii presented in Table 6 are consistent with those calculated from the PP RCS (Table 4) for individual objects.

Summary

We have described how 11 constituents of an anomalous orbital debris population, believed to be leaked NaK reactor coolant from Soviet RORSATs, were located and characterized. The initial search for anomalous debris showed that no recent leak from the putative parent satellites had been detected. This is consistent with NASA's inference that the leaks occurred soon after the nuclear power sources were placed in their disposal orbits.[18] We found that the debris tend to cluster in several orbit planes with many pieces of varying sizes in each plane. This is a key point in the analysis, and we believe these features are consistent with a leaking liquid. We have also presented observations and analysis of radar and optical data taken on most of these objects. Our analysis of the radar data has shown the following:

1) The debris found and tracked are in very similar orbits to the putative parents.

2) The tracked debris exhibit, without exception, a radar polarization ratio at all aspect angles indicative of a spherical shape.

3) The tracked debris have radii varying between 1.6 and 2.8 cm as derived from the RCSs. We note that this range in radius represents the detection limit of the MHR at the lower end and, perhaps, the largest size of the anomalous debris at the upper end.

4) The tracked debris have a mean density of 1.03 g/cm^3, which is consistent with eutectic NaK at typical orbital temperatures.

5) The photometric phase functions on 7 of the 11 objects are similar to that from a specular sphere, which is unusual for typical (nonanomalous) orbital debris.

6) The optical polarization is consistently low for all of these objects; there is no evidence of the high polarization, which is appropriate for dielectric surfaces. Hence, these objects appear to have metallic surfaces.

7) The calculated surface reflectance is high (>0.8) and is consistent with a specularly reflecting metallic surface.

8) The debris appear to have radii between 1.8 and 3.0 cm as derived from the photometric and polarimetric observations. These sizes are consistent with the radar data.

Conclusions

We conclude that the properties of this sample of the anomalous orbital debris population are consistent with the hypothesis that they result from the leak of NaK coolant from Soviet RORSATs, although the assertion is not unambiguously proven. This paper has also demonstrated a powerful capability for remote sensing and characterization of orbital debris using the MIT Lincoln Laboratory ground-based radar and optical systems.

References

[1] Stansbery, E. G., Settecerri, T. J., Matney, M. J., Zhang, J., and Reynolds, R., "Haystack Radar Measurements of the Orbital Debris Environment; 1990–1994," NASA Johnson Space Center, TR-27436, April 1996.

[2] Stansbery, E. G., Settecerri, T. J., Matney, M. J., and Reynolds, R., "Haystack Radar Measurements of the Orbital Debris Environment," NASA Johnson Space Center, TR-26655, May 1994.

[3] Stansbery, E. G., et al., "Orbital Debris Studies Using the Haystack Radar," *Proceedings of the 1995 Space Surveillance Workshop*,

Massachusetts Inst. of Technology, Lincoln Lab., Lexington, MA, 1995.

[4]Pearce, E. C., Blythe, M. S., Gibson, D. M., and Trujillo, P. J., "Space Debris Measurements: Phase One Final Report," *Proceedings of the 1994 Space Surveillance Workshop*, Massachusetts Inst. of Technology, Lincoln Lab., Lexington, MA, 1994, pp. 125–134.

[5]Sridharan, R., Gaposchkin, E. M., Moore, T. G., and Swezey, L. W., "Debris Characterization: An Interesting Example," *Proceedings of the 1996 Space Surveillance Workshop*, Massachusetts Inst. of Technology, Lincoln Lab., Lexington, MA, 1996, pp. 57–68.

[6]LeClair, R., et al., "Improvements in TRADEX Debris Capabilities," 1996 Space Surveillance Workshop, Massachusetts Inst. of Technology, Lincoln Lab., Lexington, MA, 1996.

[7]Sridharan, R., "Characteristics of Debris and Implications for Detection and Tracking," American Astronautical Society, Paper 96-117, Feb. 1996.

[8]Ruck, G. T. (ed.), *Radar Cross-Section Handbook*, Plenum, New York, 1970, p. 148.

[9]Hedin, A. E., "A Revised Thermospheric Model Based on Mass Spectrometer and Incoherent Scatter Data: MSIS83," *Journal of Geophysical Research A*, Vol. 88, No. A12, 1983, p. 10,170.

[10]Gaposchkin, E. M., and Coster, A. J., "Analysis of Satellite Drag," *Lincoln Laboratory Journal*, Vol. 1, 1988, p. 203.

[11]Gaposchkin, E. M., and Coster, A. J., "Evaluation of Recent Atmospheric Density Models," *Advances in Space Research*, Vol. 6, No. 9, 1986, p. 157.

[12]Marcos, F. A., "Accuracy of Atmospheric Drag Models at Low Satellite Altitude," *Advances in Space Research*, Vol. 10, 1990, p. 417.

[13]Miller, R. R., *Liquid Metals Handbook, Sodium (NaK) Supplement*, edited by C. B. Jackson, Atomic Energy Commission and Dept. of the Navy, Washington, DC, 1955.

[14]Gaposchkin, E. M., "Calculation of Satellite Drag Coefficients," Massachusetts Inst. of Technology, Lincoln Lab., TR 998, Lexington, MA, July 1994.

[15]Allen, C. W., *Astrophysical Quantities*, Athlone, London, 1983, pp. 201, 202.

[16]Hecht, E., *Optics*, Addison–Wesley, Reading, MA, 1988.

[17]Williams, J. G., and McCue, G. A., "An Analysis of Satellite Optical Characteristics Data," *Planetary and Space Science*, Vol. 14, 1966, p. 839.

[18]Kessler, D. J., Matney, M. J., Reynolds, R. C., Bernhard, R. P., Stansbery, E. G., Johnson, N. L., Potter, A. E., and Anz-Meador, P. D., "The Search for a Previously Unknown Source of Orbital Debris: The Possibility of a Coolant Leak in Radar Ocean Reconnaissance Satellites," NASA Johnson Space Center, TR-27737, Feb. 1997.

A. C. Tribble
Associate Editor